

**This is a self-archived version of an original article. This version may differ from the original in pagination and typographic details.**

**Author(s):** Korpisalo, P; Karvinen, H; Rissanen, T T; Kilpijoki, J; Marjomäki, Varpu; Baluk, P; McDonald, D M; Cao, Y; Eriksson, U; Alitalo, K; Ylä-Herttuala, S

**Title:** Vascular endothelial growth factor-A and platelet-derived growth factor-B combination gene therapy prolongs angiogenic effects via recruitment of interstitial mononuclear cells and paracrine effects rather than improved pericyte coverage of angiogenic vessels

**Year:** 2008

**Version:** Accepted version (Final draft)

**Copyright:** © 2008, Wolters Kluwer Health

**Rights:** In Copyright

**Rights url:** <http://rightsstatements.org/page/InC/1.0/?language=en>

**Please cite the original version:**

Korpisalo, P., Karvinen, H., Rissanen, T.T., Kilpijoki, J., Marjomäki, V., Baluk, P., McDonald, D. M., Cao, Y., Eriksson, U., Alitalo, K., & Ylä-Herttuala, S. (2008). Vascular endothelial growth factor-A and platelet-derived growth factor-B combination gene therapy prolongs angiogenic effects via recruitment of interstitial mononuclear cells and paracrine effects rather than improved pericyte coverage of angiogenic vessels. *Circulation research*, 103, 1092-1099.  
<https://doi.org/10.1161/CIRCRESAHA.108.182287>



Published in final edited form as:

*Circ Res.* 2008 November 07; 103(10): 1092–1099. doi:10.1161/CIRCRESAHA.108.182287.

## VEGF-A and PDGF-B combination gene therapy prolongs angiogenic effects via recruitment of interstitial mononuclear cells and paracrine effects rather than improved pericyte coverage of angiogenic vessels

Petra Korpisalo<sup>1</sup>, Henna Karvinen<sup>1</sup>, Tuomas T. Rissanen<sup>1</sup>, Johanna Kilpijoki<sup>1</sup>, Varpu Marjomäki<sup>2</sup>, Peter Baluk<sup>3</sup>, Donald M. McDonald<sup>3</sup>, Yihai Cao<sup>4</sup>, Ulf Eriksson<sup>5</sup>, Kari Alitalo<sup>6</sup>, and Seppo Ylä-Herttuala<sup>1,7,8</sup>

<sup>1</sup>Department of Molecular Medicine, A.I. Virtanen Institute, University of Kuopio, Finland

<sup>2</sup>Department of Biological and Environmental Science, Nanoscience center, University of Jyväskylä, Finland <sup>3</sup>Cardiovascular Research Institute, Comprehensive Cancer Center, and Department of Anatomy, University of California, San Francisco, California, USA <sup>4</sup>Microbiology and Tumor Biology Center Karolinska Institute, Stockholm, Sweden <sup>5</sup>Ludwig Institute for Cancer Research, Stockholm, Sweden <sup>6</sup>Biomedicum, University of Helsinki, Finland <sup>7</sup>Department of Medicine, University of Kuopio, Finland <sup>8</sup>Gene Therapy Unit, Kuopio University, Kuopio, Finland

### Abstract

Vessel stabilisation and the inhibition of side-effects such as tissue edema are essential in angiogenic gene therapy. Thus, combination gene transfers (GT) stimulating both endothelial cell and pericyte proliferation have become of interest. However, there is currently little data to support combination GT in large animal models. In this study we evaluated the potential advantages of such a strategy by combining the transfer of adenoviral (Ad) vascular endothelial growth factor A (VEGF-A) and platelet derived growth factor B (PDGF-B) into rabbit hindlimb skeletal muscle. AdLacZ alone or in combination with AdVEGF-A were used as controls. Contrast-enhanced ultrasound, modified Miles assay and immunohistology were used to quantify perfusion, vascular permeability and capillary size, respectively. Confocal microscopy was utilized in the assessment of pericyte-coverage. The transfer of AdPDGF-B alone and in combination with AdVEGF-A induced prominent proliferation of  $\alpha$ -sma-, CD31-, RAM11-, HAM56-, and VEGF- positive cells. Although, pericyte recruitment to angiogenic vessels was not improved, combination GT induced a longer-lasting increase in perfusion in both intact and ischemic muscles than AdVEGF-A GT alone. In conclusion, intramuscular delivery of AdVEGF-A and AdPDGF-B, combined, resulted in a prolonged angiogenic response. However, the effects were most likely mediated via paracrine mechanisms rather than an increase in vascular pericyte coverage.

Address for correspondence and reprint requests: Seppo Ylä-Herttuala MD, PhD, FESC, Department of Molecular Medicine, A.I. Virtanen Institute, University of Kuopio, P.O. Box 1627, FIN-70211 Kuopio, Finland, Phone: +358-17-162075, Fax: +358-17-163751, Seppo.Ylaherttuala@uku.fi.

### Disclosures

None.

## Keywords

angiogenesis; vascular endothelial growth factor; platelet derived growth factor; gene therapy

---

## Introduction

The stabilization of angiogenic vessels through pericyte recruitment is regarded to be essential for the maintenance of blood flow after angiogenic gene therapy of ischemic diseases.<sup>1</sup> Thus, a gene transfer (GT) that combines vascular endothelial growth factors (VEGFs) and platelet-derived growth factors (PDGFs) and stimulates both endothelial cells and pericytes could be more effective than application of single therapies.

VEGF-A is a strong endothelial mitogen that can induce efficient vascular growth and perfusion.<sup>2</sup> PDGF-B mediates pericyte proliferation and migration and is thus associated with vessel stabilization.<sup>3</sup> Interestingly, our previous studies have shown that pericyte proliferation can also be induced after transduction with adenoviral (Ad) VEGFs alone, likely, through indirect mechanisms including increased capillary pressure, shear stress and up-regulation of other growth factors.<sup>2,4</sup> Thus, actual benefits of the combination GT on pericyte proliferation and vascular recruitment associated to therapeutic angiogenesis are unclear.

Currently, very little data is available on combination GT in large animal models. Intramuscular injection of adenoviruses is currently the most efficient method for gene delivery in large animals and holds promise for clinical trials. We compared the effects of intramuscular GT of AdVEGF-A or AdPDGF-B alone or in combination on pericyte activation and the stability of angiogenic vessels in normoxic and ischemic rabbit hindlimbs. We found that the combination GT prolonged angiogenic effects although pericyte coverage of the neovessels was not enhanced. Rather, AdPDGF-B GT alone or in combination with AdVEGF-A induced recruitment of mononuclear, interstitial cells expressing endogenous VEGF.

## Materials and Methods

### Ischemia operation and gene transfers

New Zealand White rabbits (mean weight 2.5–3kg, total n=141,) received intramuscular (i.m.) injections of adenoviruses ( $10^{11}$ vp) encoding human VEGF-A<sup>165</sup> or human PDGF-B. A total dose of  $2 \times 10^{11}$ vp was used for the AdVEGF-A+AdPDGF-B combination GT.  $\beta$ -galactosidase marker gene (LacZ) alone or in combination with AdVEGF-A was used as a control. Human clinical grade, first generation, serotype 5, replication-deficient adenoviruses produced under GMP conditions and analyzed to be free from contaminants were used.<sup>4</sup> Intramuscular (i.m.) GTs were performed into the semimembranosus muscle of the thigh using a 1ml syringe and a 25-gauge needle ( $10^{11}$ vp/ml divided into 10 separate 0.1ml injections) during medetomidin (Domitor, 0.3mg/kg, Orion) and ketamin (Ketalar, 20mg/kg, Pfizer) anesthesia. Ligation of the profound femoral artery was done to a subgroup of animals (n=58) before gene transfers as previously described.<sup>2</sup> Animals were sacrificed at 6,

14 or 28 days after GT. To reduce the number of animals, the AdVEGF+AdLacZ control was not used in ischemic animals since the results did not statistically differ from transfer of AdVEGF alone to normoxic muscle. All animal experiments were approved by the Experimental Animal Committee at the University of Kuopio.

### **Contrast-enhanced ultrasound imaging of perfusion**

Perfusion in transduced and contralateral intact rabbit semimembranosus muscles was quantitatively measured with Acuson Sequoia 512 and 15L8 transducer (Siemens), using the power Doppler mode and the administration of a contrast agent 6, 14 or 28 days after GT.<sup>2</sup> Two consecutive longitudinal plane video clips of 10s (power Doppler at 8.5MHz, dynamic range 10dB, power -18dB, mechanical index 0.6, gain 40 and depth 20mm) were captured starting immediately upon a bolus injection containing 0.3ml of second generation contrast agent (sulphur hexafluoride in a phospholipid shell, approx.  $2 \times 10^8$  bubbles/ml, mean diameter 2.5 $\mu$ m, Sonovue, Bracco) into the ear vein. The perfusion ratio, was calculated with Datapro 2.13 (Noesis), using the maximum signal intensities of the transduced and contralateral intact limbs.<sup>2;5</sup> Ultrasound measurements and the analysis of data were done in a blinded manner.

### **The Modified Miles assay for the evaluation of tissue edema**

The Modified Miles assay was used for the evaluation of tissue edema at sacrifice. Evans Blue dye (30mg/kg, Sigma) was injected intra-venously 30min before sacrifice. After sacrifice, the animals were perfusion-fixed with 1L of 1% paraformaldehyde (PFA) in 0.05M citrate buffer (pH 3.5) via the left ventricle. Extravasated Evans Blue dye bound to plasma proteins (mostly albumin) was extracted from transduced and contralateral intact semimembranosus muscle samples by incubation in formamide at 60°C for 48h. The amount of extravasated Evans Blue dye was determined on the basis of absorbance at 610nm.<sup>4</sup> The results are represented as absorbance ratios between the transduced and contralateral intact muscles. The absorbances were normalized to the weight of the muscle sample.

### **Immunohistology**

The Avidin-biotin-HRP system (Vector Laboratories) with 3'-5'-diaminobenzidine (DAB, Zymed) color substrate or fluorescein isothiocyanate (FITC, Zymed) fluorescent dye was used for immunocytochemistry on 7  $\mu$ m thick paraffin-embedded sections fixed in 4% paraformaldehyde/15% sucrose for 4h. Intra-arterially injected Rhodamine-labelled Ricinus Communis lectin (1mg in 2ml of saline administered into the profound femoral artery, Vector) and FITC-conjugates were used for immunocytochemistry on 50  $\mu$ m thick frozen sections. The endothelium was immunostained using a mouse monoclonal antibody (mAb) against CD31 (DAKO, dilution 1:50). Pericytes and SMCs were stained with an  $\alpha$ -smooth muscle actin mAb ( $\alpha$ -sma, Sigma, 1:250), macrophages were stained with a mAb against rabbit macrophages (RAM11, DAKO, 1:200) and mAb against human macrophages and monocytes (HAM56, DAKO, 1:500) with a trypsin pre-treatment. Fibroblasts were identified with desmin and vimentin (Sigma, 1:100 and 1:50, respectively). Protein expressions were studied using a hVEGF antibody (Santa Cruz, 1:500) and a PDGF antibody (R&D, 1:500) with a citrate buffer boiling treatment. Receptor stainings were performed using VEGFR-1 (Santa Cruz, 1:250), VEGFR-2 (RDI, 1:250) and PDGFR- $\beta$

(Santa Cruz, 1:200) antibodies. General histology and cell morphology were studied using hematoxylin-eosin stainings. Double immunostainings comprising Avidin-biotin-HRP system with FITC (x) and anti-mouse-Alexa 546 (x) were used for the detection of VEGF and HAM56, respectively.

Photographs of the 7  $\mu\text{m}$  thick histological sections were taken with an Olympus AX70 microscope (Olympus Optical) and analySIS software (Soft Imaging System). Fluorescent images in Figure 4. were taken using an Olympus U-RFL-T burner. Confocal images of the 50  $\mu\text{m}$  thick sections were taken with an Olympus IX81 microscope and a Fluoview-1000 confocal setup. Reconstructions of the confocal images were done with an open source software package, BioImageXD.<sup>6</sup> Images were further processed for publication with Adobe Photoshop 7.0 (Adobe).<sup>4</sup>

### **Blood vessel measurements**

The mean capillary area ( $\mu\text{m}^2$ ) was measured, at 200 $\times$  magnification, from CD31 immunostained sections of semimembranosus muscles obtained from areas covered entirely by skeletal muscle tissue.<sup>4</sup> All measurements were performed in a blinded manner from 10 fields representing maximal angiogenic effects of each muscle section using analySIS software (Soft Imaging System). To avoid ambiguous data caused from trauma effects of the needle injection, the analysis was made outside the needle track area. Means of the measurements are reported. Total area of arteries and veins (% of the total muscle area) was quantified from  $\alpha$ -sma stained sections of semimembranosus muscles at 40 $\times$  magnification covering the entire muscle.

### **Measurements of $\alpha$ -sma positive cells**

The percentage of  $\alpha$ -sma positive pericytes, SMCs and myofibroblasts (% of the skeletal muscle area) were measured by immunofluorescence (FITC) of  $\alpha$ -sma-stained sections of semimembranosus muscles at 200 $\times$  magnification. All measurements were performed, using analySIS software (Soft Imaging System), in a blinded manner from 5 fields that represented maximal  $\alpha$ -sma immunofluorescence of each muscle section. Measurements were taken from areas that did not contain large arteries or veins since their SMC layer could affect the results.

### **Quantification of VEGF-A and PDGF-B protein expressions**

Muscle samples taken at sacrifice were frozen in liquid nitrogen and stored at  $-70^\circ\text{C}$ . T-Per buffer (Thermo Scientific) with 1 $\times$  Halt protease inhibitor (Thermo Scientific) was used for protein extraction from homogenized muscle samples. The amount of protein in each sample was quantified with hVEGF-A and hPDGF-B enzyme-linked-immuno-sorbent-assay (R&D Systems) and further normalized to the amount of total protein in each protein extract. The amount of total protein in each sample was quantified with BCA protein assay kit (Thermo Scientific).

## Statistical analyses

The results are expressed as the mean + SEM. Statistical significance was evaluated using the Kruskal-Wallis test followed by the Mann-Whitney U-test where appropriate.  $P < 0.05$  was considered statistically significant.

## Preparation of supplementary video files

3D reconstructions of the confocal images were prepared with Imaris-software (Bitplane). In case the video files cannot be viewed, the latest Microsoft (or equivalent) Media Player may be downloaded from <http://www.microsoft.com/windows/windowsmedia/default.mspx> or, <http://www.microsoft.com/windows/windowsmedia/software/Macintosh/osx/default.aspx> for Mac users.

## Results

### AdPDGF-B induces recruitment of interstitial cells six days after gene transfer

The efficacy of the gene transfers was confirmed using protein expression analysis of the muscle samples (see Online Figure I for results). The effect of AdPDGF-B overexpression was first studied in normoxic muscles (Figure 1). AdLacZ transduced control muscles displayed normal skeletal muscle morphology with small capillaries (Figure 1a, red arrowheads) and the occasional  $\alpha$ -sma positive pericytes surrounding the capillaries (Figure 1a, black arrowheads). The main response to AdPDGF-B transduction was the instead of angiogenesis, proliferation of cells in the muscle interstitium (Figure 1b, black arrows). Some enlarged capillaries (Figure 1b, red arrowheads), with increased pericyte coverage, (Figure 1b, black arrowheads) were also detected. AdVEGF-A induced abundant capillary enlargement (Figure 1c, red arrowheads) and recruited pericytes around the angiogenic capillaries (Figure 1c, black arrowheads). The AdVEGF-A+AdLacZ controls manifested similar histology to that of AdVEGF-A alone; only a minor recruitment of inflammatory cells, due to increased viral dosage, was observed (Figure 1d). In contrast, both the enlargement of capillaries and strong proliferation of interstitial cells (Figure 1e, black arrows) were visible after AdVEGF-A+AdPDGF-B GT. However, recruitment of pericytes to angiogenic vessels was impaired compared to AdVEGF-A or AdVEGF-A+AdLacZ (Figure 1c–e). Many  $\alpha$ -sma positive cells (Figure 1e, asterisk) and some CD31 positive cells (Figure 1e, red arrows) could be seen in the interstitium of AdVEGF-A+AdPDGF-B transduced muscles. For AdVEGF-A+dPDGF-B combination GT, two doses were tested;  $2 \times 10^{11}$ vp and  $10^{11}$ vp. However, both doses yielded similar results (see also Online Figure II for the comparison of results obtained from each dose).

The results for normoxic and ischemic animals were very similar when quantified (see also Online Figure III for histology from the ischemic muscles). AdPDGF-B alone could not induce significant changes in capillary size (Figure 2a) but moderately increased perfusion in normoxic conditions (Figure 2b). In both normoxic and ischemic muscles AdVEGF-A, AdVEGF-A+AdLacZ or AdVEGF-A+AdPDGF-B significantly increased both capillary size and perfusion when compared to AdLacZ alone (Figure 2a–b). AdVEGF-A+AdPDGF-B induced more moderate changes when compared to AdVEGF-A alone or combined with AdLacZ, which is probably explained by the moderately lower VEGF expression levels after

the combination GT (See Online Figure I). AdPDGF-B could not reduce AdVEGF-A-induced edema formation but rather even enhanced it in the ischemic muscles (Figure 2c).

### **Angiogenesis induced by AdPDGF-B or AdVEGF-A+AdPDGF-B persists longer than that stimulated by AdVEGF-A alone**

Normal skeletal muscle perfusion was detected with contrast-enhanced ultrasound in AdLacZ transduced normoxic muscles six days after GT (Figure 3a). There was a large increase in perfusion after AdVEGF-A, AdVEGF-A+AdLacZ and AdVEGF-A+AdPDGF-B GTs (Figures 3c–e) but only a small increase after AdPDGF-B GT (Figure 3b). Tissue edema was observed between semimembranosus and gracilis muscles in all AdVEGF-A, AdVEGF-A+AdLacZ and AdVEGF-A+AdPDGF-B (Figure 3c–e, asterisks). 14 days after GT perfusion increases induced by AdVEGF-A and AdVEGF-A+AdLacZ were decreased to baseline (Figure 3h–I). However, perfusion increases induced by AdPDGF-B and AdVEGF-A+AdPDGF-B were still visible (Figures 3g and j, see also Supplementary video 1). Tissue edema was also still detectable in AdVEGF-A+AdPDGF-B 14 days after GT (Figure 3h, asterisk).

In addition to the ultrasound findings, the analysis of CD31 stained muscle sections 14 days after GT (Figure 3k–o,q) revealed that histological changes induced by AdPDGF-B alone or in combination had also persisted. For AdVEGF-A or AdVEGF-A+AdLacZ most vessels had regressed, although there were, some regressing vascular structures, still visible (Figure 3m–n, arrowheads). However, in AdPDGF-B and AdVEGF-A+AdPDGF-B transduced muscles large arteries and veins, and, to some extent capillaries, were still enlarged (Figure 3l and o, arrows). Also, cell density was still increased in the muscle interstitium and often localized to persistent angiogenic vessels (Figure 3l and o, asterisks).

Quantification of the ultrasound data displayed dramatic changes in skeletal muscle perfusion induced by the GTs (Figure 3p). Whereas perfusion in AdVEGF-A and AdVEGF-A+AdLacZ transduced muscles quickly decreased after 6 days, a statistically significant increase in perfusion was still observed 14 days after AdVEGF-A+AdPDGF-B GT in both intact and ischemic muscles (Figure 3p). AdPDGF-B transduced muscles showed very little attenuation of the effect and ischemic muscles had increased perfusion even 28 days after GT. Ultrasound findings on day 14 were supported by quantification of the histological findings on the same time point yielding significant increases in vascularity in AdPDGF-B and AdVEGF-A+AdPDGF-B transduced muscles (Figure 3q).

### **AdPDGF-B induces proliferation of $\alpha$ -sma positive pericytes and fibroblasts, and induces recruitment of CD31-, HAM56- and VEGF-positive cells**

As expected, AdPDGF-B induced a significant proliferation of  $\alpha$ -sma positive cells in rabbit skeletal muscle six days after GT (Figure 4a). However, not all cells in the muscle interstitium were positive for  $\alpha$ -sma. Thus, a series of immunostainings were done to investigate which cells accumulated in AdPDGF-B transduced muscles. Cell proliferation was confirmed using Ki67 staining (Figure 4b). Hematoxylin-Eosin staining allowed the identification of fibroblasts (Figure 4c, arrow) and some granulocytes (Figure 4c, arrowhead). Desmin and Vimentin stainings were also performed to confirm the presence of

fibroblasts (data not shown). The occasional presence of macrophages was detected with RAM11 staining (Figure 4d, arrowhead). HAM56 staining showed more positivity as it also stained monocytes in addition to macrophages (Figure 4e). CD34 only stained the vascular endothelium of large arteries in the samples (Figure 4f). However CD31 also stained some extravascular cells in the muscle interstitium (Figure 4g, arrows) in addition to endothelial cells (Figure 4g, arrowheads). The expression of VEGF was detected in the blood vessel endothelium (Figure 4h, arrows), fibroblasts and several mononuclear cells (Figure 4h, arrowheads) of AdPDGF-B transduced muscles. Where as vascular structures only displayed a weak PDGF-B expression (Figure 4i, red arrows), strong expression could be found in individual cells in the interstitium (Figure 4i, arrowheads) and in the extracellular matrix (Figure 4i, black arrow). A double staining for VEGF and HAM56 confirmed that VEGF was expressed by HAM56 positive macrophages and monocytes (Figures 4j-l, arrows display co-localized staining). VEGFR-1 expression was found in the vascular endothelium (Figure 4m, arrowheads) and in the interstitial cells (Figure 4m, arrows). Additionally, VEGFR-2 and PDGFR- $\beta$  expression was found in the interstitial cells (Figure 4n-o, arrows).

### **The recruitment of $\alpha$ -sma positive pericytes to vessels is impaired in AdVEGF-A+AdPDGF-B transduced muscles**

Quantification of  $\alpha$ -sma positive cells from histological samples revealed that AdPDGF-B induced a small but significant proliferation of  $\alpha$ -sma positive cells in normoxic muscles compared to the AdLacZ control six days after GT (Figure 5a). In contrast, AdVEGF-A, AdVEGF-A+AdLacZ and AdVEGF-A+AdPDGF-B showed highly increased numbers of  $\alpha$ -sma positive cells in the muscle. No significant difference was observed between AdVEGF-A, AdVEGF-A+AdLacZ and AdVEGF-A+AdPDGF-B (Figure 5a). However, confocal images of the transduced muscles with Rhodamine lectin (endothelium in red) infusion and  $\alpha$ -sma immunostaining (pericytes in green) demonstrated that the recruitment of pericytes to angiogenic vessels differed between the two groups. In AdVEGF-A transduced muscles  $\alpha$ -sma positive pericytes were closely associated with enlarged capillaries (Figure 5b, see also Supplementary video 2). After AdVEGF-A+AdPDGF-B GT, large numbers of  $\alpha$ -sma positive cells were not associated with vessels but were scattered in the muscle interstitium (Figure 5c, asterisks, see also Figure 1d). These cells also possessed long extensions projecting away from the vessels (Figure 5c, arrowheads, see also Supplementary video 3).

## **Discussion**

Adenoviral delivery of VEGFs is a potentially useful way to increase perfusion in ischemic muscles. The main problems of AdVEGF-A GT include increased plasma protein extravasation leading to tissue edema and the instability of the newly formed vessels.<sup>1;2;4</sup> PDGFs induce pericyte recruitment and migration, and are thus proposed to stabilize vessels and decrease edema.<sup>7-9</sup> In this study, we tested the effect of intramuscular AdPDGF-B in combination with AdVEGF-A on vessel stability and edema formation in intact and ischemic rabbit skeletal muscles.

Rather than inducing angiogenesis, AdPDGF-B GT induced the proliferation of  $\alpha$ -sma positive pericytes and fibroblasts and the accumulation of interstitial cells, including

inflammatory cells such as monocytes, in both normoxic and ischemic muscles, six days after GT. Occasional enlargement of capillaries was detected near the interstitial cells in AdPDGF-B transduced muscles, possibly indicating a role for the interstitial cells in the angiogenic process as previously described.<sup>10</sup> Capillary enlargement after AdPDGF-B GT was more visible in ischemic animals. However, as capillary size was also increased in the ischemic AdLacZ controls, the increase was most likely mediated by hypoxia regulated endogenous growth factors. In contrast, AdVEGF-A induced efficient angiogenesis and recruitment of pericytes around growing vessels at six days. However, as expected extensive tissue edema accompanied rapid changes in vascular growth. When the two growth factors were combined both angiogenesis and massive proliferation of interstitial cells were observed. The mean capillary area and perfusion were smaller in AdVEGF-A+AdPDGF-B transduced muscles compared to AdVEGF-A alone or AdVEGF-A+AdLacZ GT in both normoxic and ischemic conditions. However, edema was rather increased than decreased in the AdVEGF-A+AdPDGF-B combination group, especially in ischemic muscles. Thus, at six days the combination GT had no significant improvement of angiogenesis and failed to reduce acute edema.

Combination GT was expected to decrease angiogenesis associated edema via stabilization of angiogenic vessels. However, further analysis of the vascular structures in AdVEGF-A and AdVEGF-A+AdPDGF-B transduced muscles showed that the recruitment of pericytes to vascular structures was impaired in the combination group compared to AdVEGF-A alone. Although the number of  $\alpha$ -sma positive cells did not differ between the groups, pericytes in the AdVEGF-A+AdPDGF-B group had projections directing away from the vascular structures. An explanation of this might be the site of transgene expression in the target tissue. In tumor studies it has been reported that PDGF secreted by tumor cells leads to abnormal attachment of pericytes to vessels.<sup>11</sup> Also, endothelial PDGF-B retention has been shown to be crucial for proper pericyte investment on the vessels during vascular growth.<sup>12</sup> We showed that following intramuscular GT, transgene production took place in several cell types including myocytes, fibroblasts and vascular cells. Our histological analysis also showed deposition of PDGF-B protein in the extracellular matrix. It is possible that overexpression of the transgene outside the vascular wall results in the lack of PDGF gradients from endothelial cells and leads to improper pericyte guidance. AdVEGF-A expression alone can induce relatively efficient pericyte recruitment even if the transgene is not expressed in the vessel wall due to blood flow and shear-stress mediated mechanisms.<sup>2;4;13</sup> In fact, the addition of exogenous PDGF-B appears to cause pericyte detachment from the vessels as shown in the confocal images of AdVEGF-A+AdPDGF-B transduced muscles. Thus, the intramuscular combination GT seems to activate pericyte migration away from the vessel wall rather than towards it. These results address the importance of proper PDGF-B gradients in target tissues in order to induce efficient pericyte recruitment on vessels.

14 days after GT, the effects of AdVEGF-A returned to baseline levels as the expression of transgene attenuated. However, in AdVEGF-A+AdPDGF-B transduced muscles, perfusion and interstitial cell density were still increased. Also, tissue edema was still observed at 14 days after AdVEGF-A+AdPDGF-B GT. Thus, although the combination GT was unable to decrease edema, it was able to induce longer lasting increases in perfusion, compared to

AdVEGF-A GT alone, in both normoxic and ischemic muscles. Interestingly, AdPDGF-B was found to induce significant recruitment of inflammatory cells and CD31-positive non-endothelial cells in the transduced muscles six and 14 days after GT. Additionally, the angiogenic changes at both time points were often found near sites of cell accumulation. Importantly, many of the interstitial cells in AdPDGF-B transduced muscle, such as monocytes and macrophages, expressed endogenous VEGF. Additionally, CD31-positive non-endothelial cells have been previously described to have angiogenic potential.<sup>14</sup> Thus, strengthening of angiogenesis via paracrine secretion of growth factors seems a plausible mechanism for the improved net effect of the combination GT and AdPDGF-B. The role of inflammatory cells in arteriogenesis<sup>10;15</sup> and bone marrow derived cells mediating PDGF-CC induced revascularization<sup>16</sup> have been suggested previously and is in line with our findings. However, the risk of fibrosis caused by the accumulation of inflammatory cells<sup>17</sup> and the immediate effect of AdPDGF-B on fibroblasts<sup>18</sup> needs to be considered against the therapeutic potential.

In summary, this study proposes that AdPDGF-B in combination with AdVEGF-A prolongs angiogenic effects via paracrine growth factors secreted from recruited cells. Additionally, this study displays the importance of proper transgene expression in target tissues in order to induce proper pericyte investment on vessels.

## Supplementary Material

Refer to Web version on PubMed Central for supplementary material.

## Acknowledgments

### Acknowledgements and Funding

This study was supported by grants from the Finnish Academy, European Union (Lymphangiogenomics LSHG-CT-2004-503573), Sigrid Juselius Foundation, the Finnish Cultural Foundation, Aarne and Aili Turunen foundation, Paavo Nurmi foundation and Emil Aaltonen foundation. This research was also supported in part by US National Institutes of Health grants HL24136 and HL59157 from the National Heart, Lung, and Blood Institute, CA82923 from the National Cancer Institute (DMcD). Technicians in the group of Molecular Medicine and at the National Experimental Animal Center of Kuopio University are acknowledged for their expertise and technical help. The authors would like to thank Dr. Roseanne Girnary PhD for linguistic revision of this manuscript and Dr. Henna Parviainen for her help in data re-analysis.

## References

1. Yla-Herttuala S, Alitalo K. Gene transfer as a tool to induce therapeutic vascular growth. *Nat Med*. 2003; 9:694–701. [PubMed: 12778168]
2. Rissanen TT, Korpisalo P, Markkanen JE, Liimatainen T, Orden MR, Kholova I, de Goede A, Heikura T, Grohn OH, Yla-Herttuala S. Blood flow remodels growing vasculature during vascular endothelial growth factor gene therapy and determines between capillary arterialization and sprouting angiogenesis. *Circulation*. 2005; 20(112):3937–3946.
3. Lindahl P, Johansson BR, Leveen P, Betsholtz C. Pericyte loss and microaneurysm formation in PDGF-B-deficient mice. *Science*. 1997; 277:242–245. [PubMed: 9211853]
4. Rissanen TT, Markkanen JE, Gruchala M, Heikura T, Puranen A, Kettunen MI, Kholova I, Kauppinen RA, Achen MG, Stacker SA, Alitalo K, Yla-Herttuala S. VEGF-D is the strongest angiogenic and lymphangiogenic effector among VEGFs delivered into skeletal muscle via adenoviruses. *Circ Res*. 2003; 92:1098–1106. [PubMed: 12714562]

5. Rissanen TT, Korpisalo P, Karvinen H, Liimatainen T, Laidinen S, Gröhn O, Ylä-Herttuala S. High-Resolution Ultrasound Perfusion Imaging of Therapeutic Angiogenesis. *Journal of American College of Cardiology: Cardiovascular Imaging*. 2008; 1:83–91.
6. Kankaanpää, P., Pahajoki, K., Marjomäki, V., Heino, J., White, D. BioImageXD. 2006. <http://www.bioimagexd.net>. Ref Type: Computer Program
7. Richardson TP, Peters MC, Ennett AB, Mooney DJ. Polymeric system for dual growth factor delivery. *Nat Biotechnol*. 2001; 19:1029–1034. [PubMed: 11689847]
8. Cao R, Brakenhielm E, Pawliuk R, Wariaro D, Post MJ, Wahlberg E, Leboulch P, Cao Y. Angiogenic synergism, vascular stability and improvement of hind-limb ischemia by a combination of PDGF-BB and FGF-2. *Nat Med*. 2003; 9:604–613. [PubMed: 12669032]
9. Uutela M, Wirzenius M, Paavonen K, Rajantie I, He Y, Karpanen T, Lohela M, Wiig H, Salven P, Pajusola K, Eriksson U, Alitalo K. PDGF-D induces macrophage recruitment, increased interstitial pressure, and blood vessel maturation during angiogenesis. *Blood*. 2004; 104:3198–3204. [PubMed: 15271796]
10. Zentilin L, Tafuro S, Zacchigna S, Arsic N, Pattarini L, Sinigaglia M, Giacca M. Bone marrow mononuclear cells are recruited to the sites of VEGF-induced neovascularization but are not incorporated into the newly formed vessels. *Blood*. 2006; 107:3546–3554. [PubMed: 16391016]
11. Abramsson A, Lindblom P, Betsholtz C. Endothelial and nonendothelial sources of PDGF-B regulate pericyte recruitment and influence vascular pattern formation in tumors. *J Clin Invest*. 2003; 112:1142–1151. [PubMed: 14561699]
12. Lindblom P, Gerhardt H, Liebner S, Abramsson A, Enge M, Hellstrom M, Backstrom G, Fredriksson S, Landegren U, Nystrom HC, Bergstrom G, Dejana E, Ostman A, Lindahl P, Betsholtz C. Endothelial PDGF-B retention is required for proper investment of pericytes in the microvessel wall. *Genes Dev*. 2003; 17:1835–1840. [PubMed: 12897053]
13. Van Gieson EJ, Murfee WL, Skalak TC, Price RJ. Enhanced smooth muscle cell coverage of microvessels exposed to increased hemodynamic stresses in vivo. *Circ Res*. 2003; 92:929–936. [PubMed: 12663481]
14. Kawamoto A, Tkebuchava T, Yamaguchi J, Nishimura H, Yoon YS, Milliken C, Uchida S, Masuo O, Iwaguro H, Ma H, Hanley A, Silver M, Kearney M, Losordo DW, Isner JM, Asahara T. Intramyocardial transplantation of autologous endothelial progenitor cells for therapeutic neovascularization of myocardial ischemia. *Circulation*. 2003; 107:461–468. [PubMed: 12551872]
15. Arras M, Ito WD, Scholz D, Winkler B, Schaper J, Schaper W. Monocyte activation in angiogenesis and collateral growth in the rabbit hindlimb. *J Clin Invest*. 1998; 101:40–50. [PubMed: 9421464]
16. Li X, Tjwa M, Moons L, Fons P, Noel A, Ny A, Zhou JM, Lennartsson J, Li H, Luttun A, Ponten A, Devy L, Bouche A, Oh H, Manderveld A, Blacher S, Communi D, Savi P, Bono F, Dewerchin M, Foidart JM, Autiero M, Herbert JM, Collen D, Heldin CH, Eriksson U, Carmeliet P. Revascularization of ischemic tissues by PDGF-CC via effects on endothelial cells and their progenitors. *J Clin Invest*. 2005; 115:118–127. [PubMed: 15630451]
17. Tzeng DY, Deuel TF, Huang JS, Baehner RL. Platelet-derived growth factor promotes human peripheral monocyte activation. *Blood*. 1985; 66:179–183. [PubMed: 2988667]
18. Bonner JC. Regulation of PDGF and its receptors in fibrotic diseases. *Cytokine Growth Factor Rev*. 2004; 15:255–273. [PubMed: 15207816]

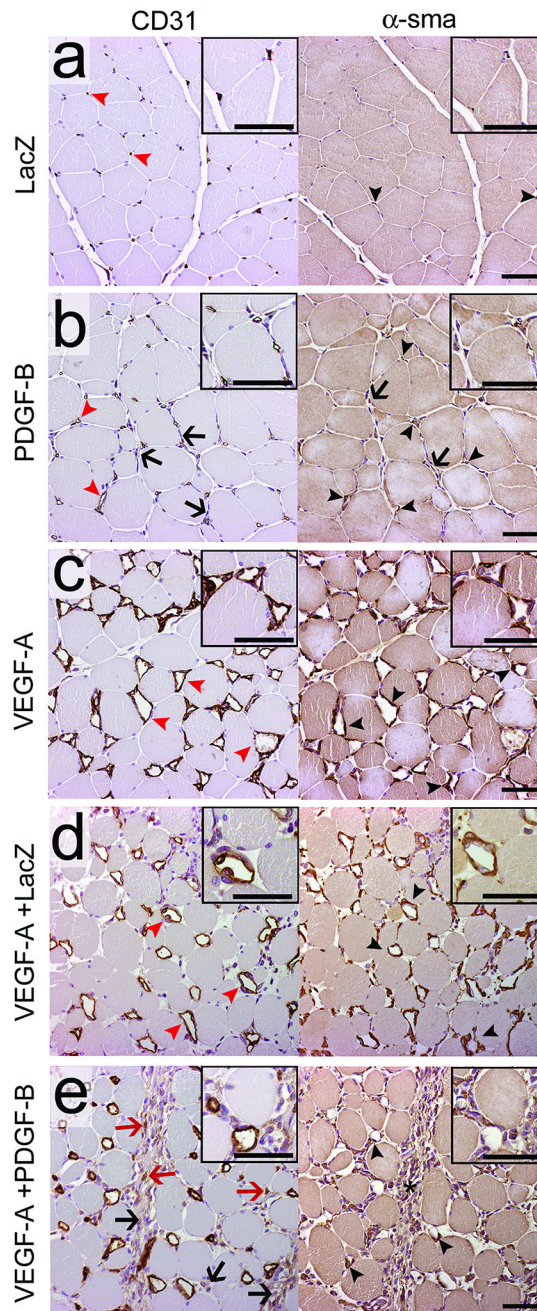


**Figure 1. AdPDGF-B alone or in combination with AdVEGF-A recruits more interstitial cells than AdVEGF-A or other controls**

CD31 (endothelium) and  $\alpha$ -sma (pericytes) stainings of serial sections of AdLacZ, AdPDGF-B, AdVEGF-A, AdVEGF-A+AdLacZ or AdVEGF-A+AdPDGF-B transduced normoxic muscles six days after gene transfer. **a)** The AdLacZ muscles have histology very similar to that of intact muscles. The capillaries (red arrowheads) are small and occasionally surrounded by pericytes (black arrowheads). **b)** AdPDGF-B induced sporadic enlargement of capillaries (red arrowheads) that acquired efficient pericyte coverage (black arrowheads), and also induced proliferation of cells in the muscle interstitium (black arrows). **c)**

AdVEGF-A induced abundant capillary enlargement (red arrowheads) and the recruitment of pericytes around the capillaries (black arrowheads). **d**) In AdVEGF-A+AdLacZ transduced muscles capillary size (red arrowheads) or pericyte recruitment (black arrowheads) of vessels did not differ from AdVEGF-A alone. **e**) In AdVEGF-A+AdPDGF-B transduced muscles both enlargement of capillaries and proliferation of interstitial cells (black arrows) were visible. However, recruitment of pericytes around angiogenic vessels was impaired compared to AdVEGF-A (black arrowheads). Several  $\alpha$ -sma positive cells (asterisk) and some CD31 positive cells (red arrows) could be seen in the interstitium. Scale bars 50 $\mu$ m.

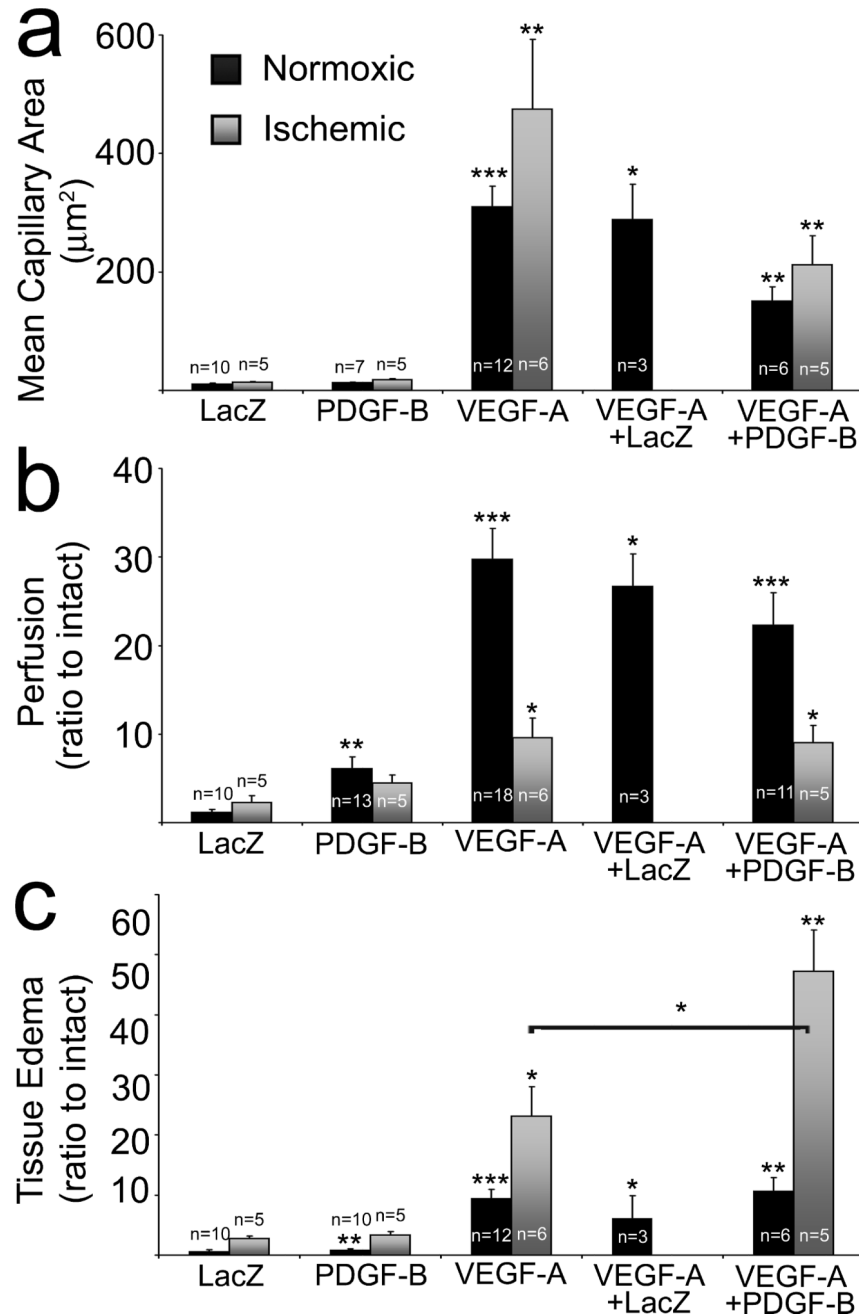


**Figure 2. Combination gene transfer with AdPDGF-B and AdVEGF-A results in more interstitial cells and more tissue edema compared to AdVEGF-A alone**  
**a)** Mean capillary size six days after different gene transfers in normoxic or ischemic muscles. AdVEGF-A, AdVEGF-A+AdLacZ and AdVEGF-A+AdPDGF-B induced significant increases in capillary size in both normoxic and ischemic muscles. In ischemic muscles the capillary size was higher than in normoxic muscles in each group. **b)** Perfusion six days after GT in normoxic and ischemic muscles. In normoxic muscles all growth factors studied induced a significant increase in perfusion compared to AdLacZ. In ischemic muscles only AdVEGF-A, AdVEGF-A+AdLacZ and AdVEGF-A+AdPDGF-B reached

statistical significance. e) Evans Blue absorbance as a measure of tissue edema in normoxic and ischemic animals six days after GT. AdVEGF-A, AdVEGF-A+AdLacZ and AdVEGF-A+AdPDGF-B significantly increased tissue edema in both normoxic and ischemic muscles. AdVEGF-A+AdPDGF-B transduced ischemic muscle had even more edema than ischemic AdVEGF-A transduced muscles. \*\*P<0.01, \*P<0.05 towards AdLacZ at the same time point unless otherwise indicated.

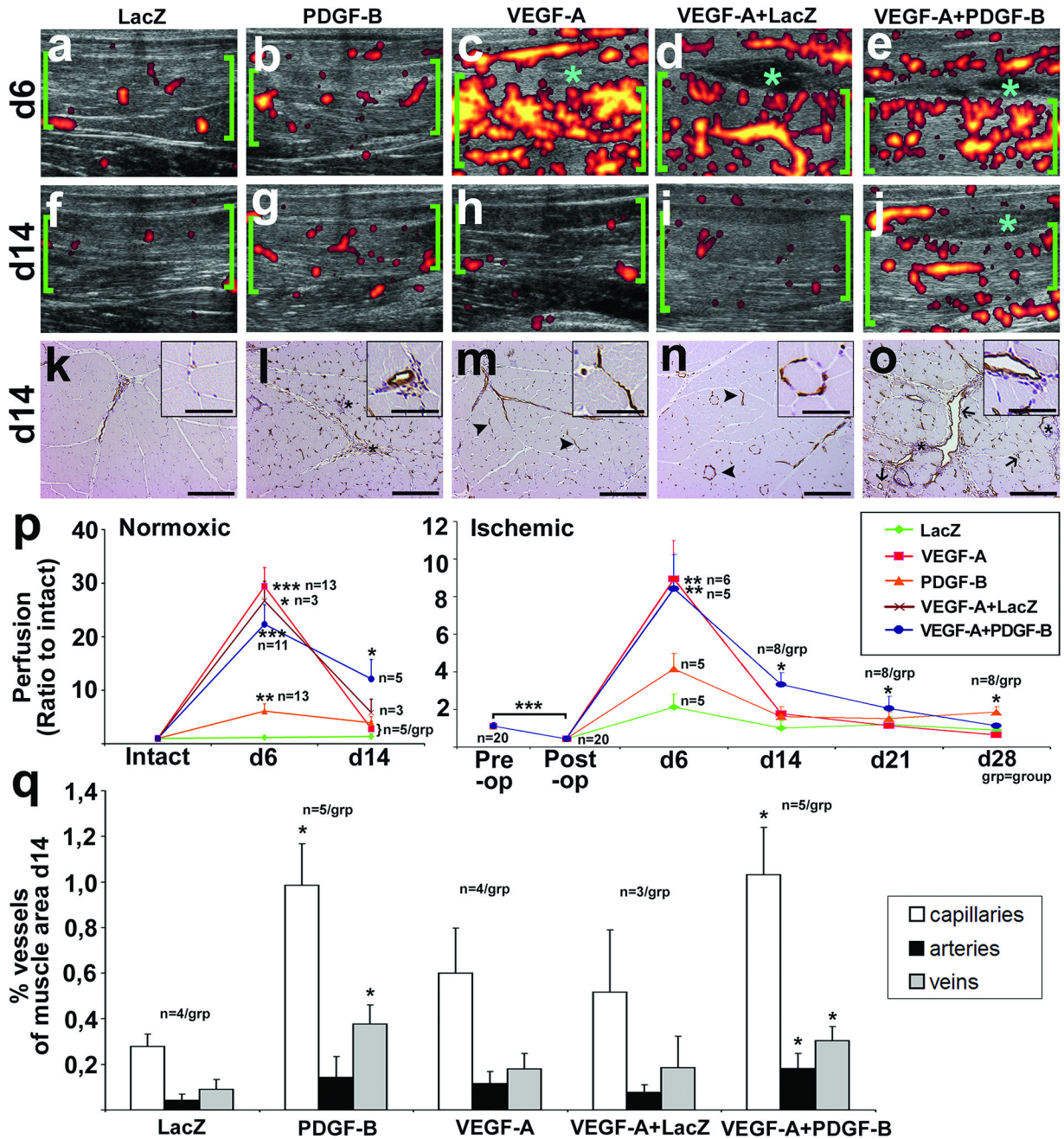


**Figure 3. Perfusion increase induced by AdPDGF-B or AdVEGF-A+AdPDGF-B is not decreased to baseline in two weeks**

Ultrasound images and histology of normoxic muscles in different study groups 1 or 2 weeks after GT. **a-e)** Contrast enhanced power Doppler ultrasound images showing perfusion in normoxic rabbit semimembranosus muscle (green brackets) six days after GT. Perfusion was highly increased in AdVEGF-A (c), AdVEGF-A+LacZ (d) and AdVEGF-A+AdPDGF-B (e), minor increase was also seen in AdPDGF-B (b). Tissue edema was observed between semimembranosus and gracilis muscles in AdVEGF-A, AdVEGF-A+AdLacZ and AdVEGF-A+AdPDGF-B (c-e, light blue asterisks). **f-j)** Ultrasound images 14 days after GT to normoxic muscle. Perfusion was decreased to baseline levels in

AdVEGF-A (h) and AdVEGF-A+AdLacZ (i). In AdPDGF-B (g) and AdVEGF-A +AdPDGF-B (j) increased perfusion was still visible. Tissue edema was still detectable in AdVEGF-A+AdPDGF-B (j, asterisk). **k–o**) CD31 immunostained histological sections of the semimembranosus muscles 14 days after GT. Scale bars 200  $\mu\text{m}$  in full images and 50  $\mu\text{m}$  in insets. **(k)** No changes due to the gene transfer were seen in AdLacZ controls. **(m–n)** Muscle morphology returned to normal also in AdVEGF-A and AdVEGF-A+AdLacZ. Some regressing vascular structures were visible (m-n, arrowheads). **(l)** In contrast, in AdPDGF-B and **(o)** AdVEGF-A+AdPDGF-B transduced muscles large arteries and veins and to some extent capillaries were still enlarged (o, arrows). Cell density was still increased in the muscle interstitium in AdPDGF-B and AdVEGF-A+AdPDGF-B transduced samples (l, o, asterisks). **p)** Quantification of the contrast enhanced ultrasound data displayed a statistically significant increase in perfusion 14 days after AdVEGF-A +AdPDGF-B in both intact and ischemic muscles. AdPDGF-B transduced muscles showed very little attenuation of the effect and the ischemic muscles still had slightly increased perfusion 28 days after GT. **q)** Quantification of histological changes in vasculature on day 14 showed a significantly higher amount of capillaries and veins in AdPDGF-B transduced muscles compared to controls. In AdVEGF-A+AdPDGF-B transduced muscles the amount of all capillaries, arteries and veins was increased compared to controls.  $**P<0.01$ ,  $*P<0.05$  towards AdLacZ at the same time point unless otherwise indicated. See also supplementary video 1 for day 14 ultrasound videos.

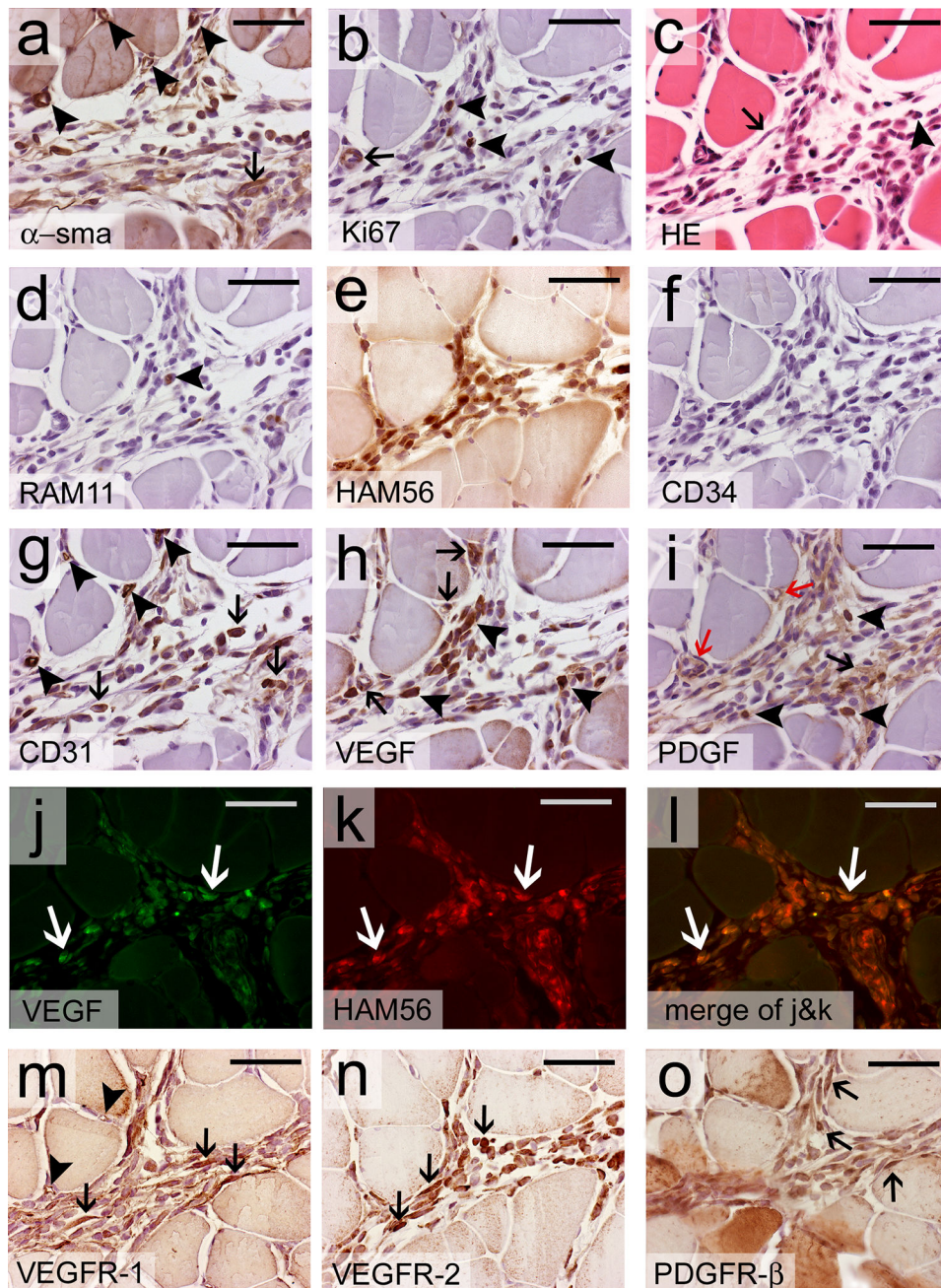


**Figure 4.**  $\alpha$ -sma, CD31, HAM56, VEGFR-1 and -2, PDGFR- $\beta$  and VEGF -positive cells were found in the muscle interstitium six days after AdPDGF-B gene transfer to normoxic muscle **a)**  $\alpha$ -sma positive pericytes could be found both around vascular structures (arrowheads) and in the interstitium (arrow) in AdPDGF-B transduced muscles. However, a large part of the proliferating cells in the muscle interstitium were not positive for  $\alpha$ -sma. **b)** Proliferation of the interstitial cells was confirmed using Ki67 staining. Ki67 positivity was found among cells in the interstitium (arrowheads) and also in vascular wall (arrow). **c)** Hematoxylin-eosin staining displayed a typical fibroblast structure in some cells (arrow) and a few cells could be identified as granulocytes based on the shape of their nuclei (arrowhead). **d)**

RAM11 positive macrophages were an example of inflammatory cells found after AdPDGF-B GT (arrowhead). **e**) Several monocytes were stained by HAM56 in addition to macrophages. **f**) CD34 only stained the endothelium of large arteries in the samples. **g**) CD31 positive cells are normally found as part of vascular structures (arrowheads) but in AdPDGF-B transduced muscles many could also be detected in the interstitium (arrows). **h**) Endogenous VEGF protein expression was detected among many of the cells in the interstitium (arrowheads) in addition to vascular cells (arrows). **i**) Strong PDGF-B protein expression was detected in a few, probably transduced cells (arrowheads). Lower expression levels were found in vascular structures (red arrows) and in the extracellular matrix (black arrow). **j**) VEGF and **k**) HAM56 double staining confirmed after **l**) merging of images that some monocytes are positive for VEGF. **m**) VEGFR-1 expression was detected in endothelium (arrowheads) and in the interstitial cells (arrows). **n**) VEGFR-2 and **o**) PDGFR- $\beta$  were also detected in the proliferating cells (arrows). Scale bars 100 $\mu$ m in all images.

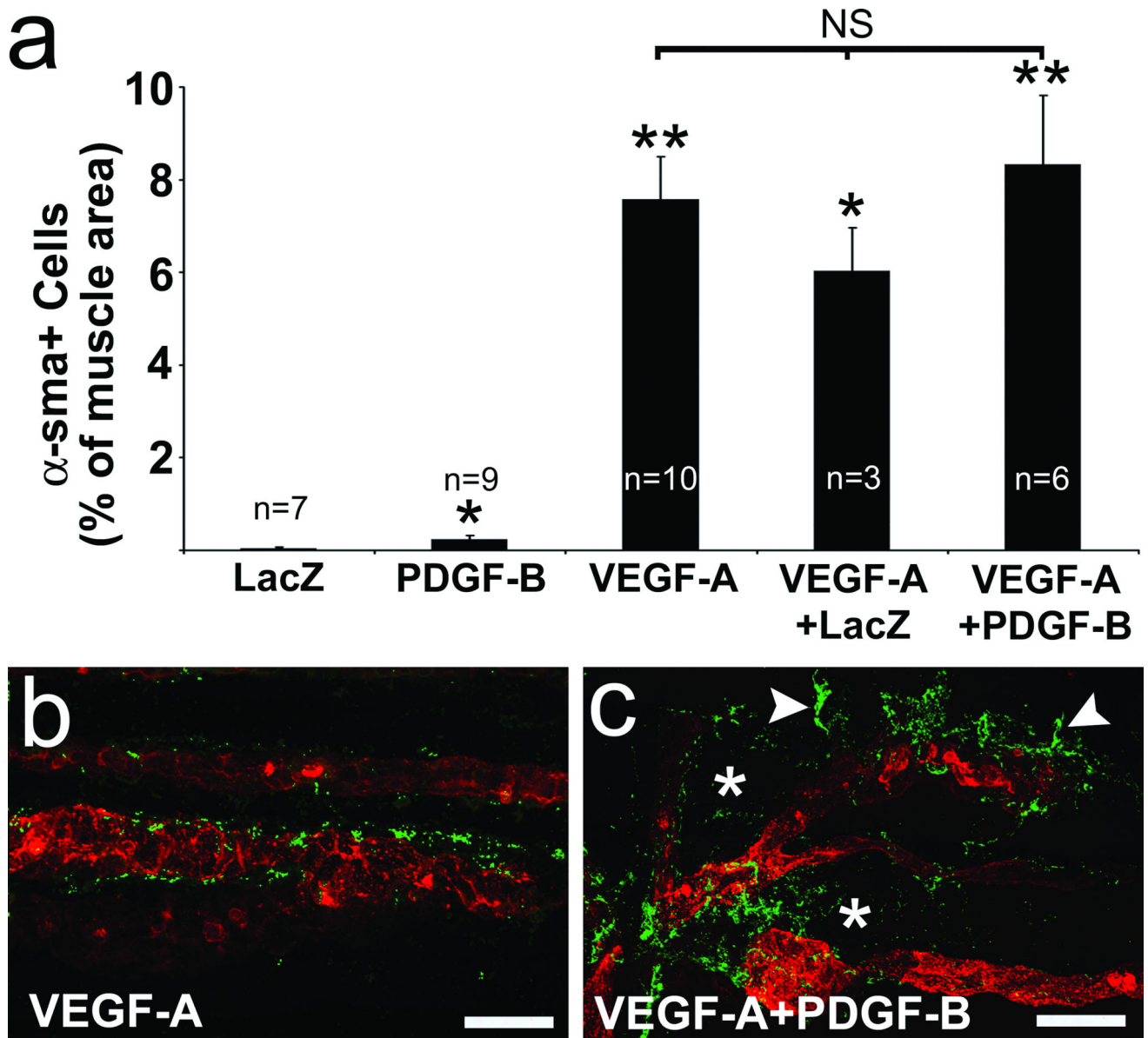


**Figure 5. AdPDGF-B increases the amount of  $\alpha$ -sma positive cells within the target muscle but the recruitment of pericytes to vascular structures is impaired**

**a)** Quantification of the amount of  $\alpha$ -sma positive cells in normoxic groups on d6 showed that AdPDGF-B increased the amount of  $\alpha$ -sma positive cells both when given alone or in combination with AdVEGF-A. **b)** In confocal images of AdVEGF-A transduced muscles  $\alpha$ -sma positive pericytes ( $\alpha$ -sma, green) were associated with vascular structures (lectin, red). **c)** In contrast,  $\alpha$ -sma positive cells could often be detected in the muscle interstitium of AdVEGF-A+AdPDGF-B transduced muscles without any association with vessels (asterisks). Also, pericytes that could be seen on vessels had long projections directed away from the vessels (arrowheads) after AdVEGF-A+AdPDGF-B GT. Scale bars in b–c 50 $\mu$ m. See 3D-animations of the confocal images in supplementary videos 2 and 3 for a more accurate picture of the vascular-pericyte interactions.